

Influence of AC Frequency, Current and Stand-Off Distance on Bead Profile in AC TIG Welding of Aluminium

ORCID: Debabrata Roy: <https://orcid.org/0009-0007-5914-7321>
ORCID: Santanu Das: <https://orcid.org/0000-0001-9085-3450>

Debabrata Roy¹ and Santanu Das²

¹Past M.Tech Student, ²Professor

Department of Mechanical Engineering, Kaiyani Government Engineering College
Kalyani- 741235, Nadia, West Bengal, India.

Email: ¹roydebu5555@gmail.com, ²sdas.me@gmail.com

DOI : 10.22486/lwj.v56i2.221110



Abstract

Using Gas Tungsten Arc Welding, or TIG Welding, good quality weld can be obtained. In this process, a shielding Gas is used to avoid atmospheric contamination of the molten weld pool. In the present work, bead profile in aluminium workpiece is observed as welded by AC TIG welding under 100% argon gas shield. Effects of variation of arc frequency, current and stand-off distance on bead profile are investigated. In the experiment, the bead-on-plate welding of 14 treatments is performed on Al 1000 series aluminium plates without a filler wire utilizing Central Composite Design system of Response Surface Methodology (RSM). Gas pressure is maintained at 2 kg/cm² with gas flow rate of 15 lit/min, welding speed of 100 mm/min, electrode diameter of 3 mm and wave balance of -25. From this investigation, it is observed that an increase in welding current increases weld penetration. These are caused by the increase in heat input with the increase in weld current and decrease in torch travel speed. An increase in stand-off distance is also observed to cause a decrease in weld penetration. Analysis of variance (ANOVA) is also performed on the observed results. Regression equations are formed relating the response to the factors (independent variables). Linear relationships are found to be quite significant for both the cases of penetration and weld bead width. Acceptable correlation coefficients (R²) more than 95% are obtained in case of depth of penetration and more than 99% in case of bead width indicating effectiveness of the results observed.

Keywords: Welding, GTAW; Aluminium, Bead-on-plate, AC frequency.

1.0 INTRODUCTION

Tungsten Inert Gas (TIG) Welding, which has the generic name of Gas Tungsten Arc Welding (GTAW), is a type of arc welding processes in which weld bead or coalescence is formed by heating the job through an electrical arc. In this process, a shielding gas (argon, helium, etc.) is used to avoid oxidation and other contamination of the molten weld pool. Arc energy produced is conducted through a column of highly ionized gas and metal vapour known as plasma [1]. GTAW is a versatile process and uses non-consumable tungsten electrode. Filler material may be added if needed. This welding is used to weld thin sections of stainless steel and nonferrous metals such as

aluminum, magnesium, and copper alloys. However, this process is slower than most other welding techniques [2]. Aluminum alloys are widely used in transportation industries, such as construction of fast boat hulls, fast trains and railway wagons, due to their light weight and resistance to corrosion. Magnesium and manganese are the major alloying elements with aluminum, and this combination has been classified a non-heat treatable alloy [3].

Aluminum alloys have wide applications [4] in many fields such as construction, transportation, and aerospace due to their excellent performance, including light weight, high strength and ductility and good corrosion resistance. The effect of pulse

current on tensile strength after TIG welding of AA6061 aluminum alloy was explored and results showed [5] that the pulse current and pulse frequency were directly proportional tensile strength, whereas base current and pulse on time had inverse relationship with tensile strength. Reddy et al. [6] investigated the effect of current pulsation frequency on weld bead, microstructure, hardness and tensile property. Results showed that the grain size of micro structure decreased with the introduction of current pulsation. Lothongkum et al. studied [7] the effects of pulsed TIG welding parameters on AISI 316l stainless steel plate. Investigation showed that increasing welding speed caused decrease in weld width and depth to width ratio.

Guang-jun et al. [8] did the experiment with variable polarity to study the weld pool by visual sensing of aluminum alloy, and the result showed that variable polarity power was less effective technique over composite filter technology to capture the better image of weld pool. Mohan et al. [9] investigated the effect of welding parameters such as welding speed and welding current on tensile strength of welding joints using aluminum as a parent metal. Results showed that welding current increased depth of welding.

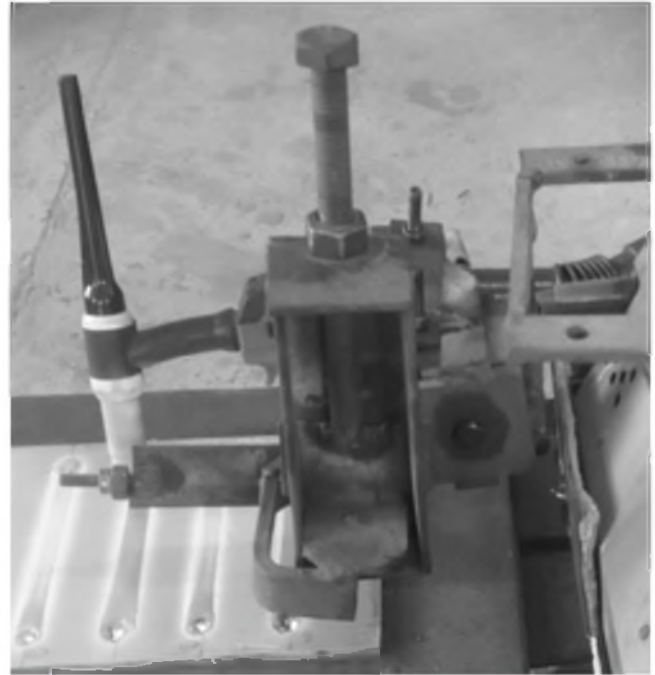


Fig. 1 : Photograph of a close view of the experimental set up

Table 1 : Chemical composition of the work piece

Si %	Fe %	Mn %	B %	V %	Pb %	Ni %	Zn %	Ti %
0.059	0.364	0.0047	0.0016	0.012	0.0037	0.0066	0.0078	0.026
Sn %	Zr %	Li %	P %	Bi %	Ce %	Co %	Ga %	Al %
0.0056	0.0016	<0.001	>0.012	0.0048	<0.0015	0.0011	0.0091	99.5

Potluri et al. [10] investigated on the effect on weld metal characteristics and significance of it on improving mechanical property in GMAW welding using Al-Zn-Mg alloy (7005) with pulsed current. Results showed that under pulsed current, welds had increased UTS and fatigue life. Fusion zone hardness was very much significant in this welding process.

Biswas et al. [11] used Al6060 alloy plates and did different experiments on bead geometry. They concluded that the increase of AC frequency decreased bead width and increased width with the increase in wave balance. Morisada et al. [12] worked with developed method of high frequency tungsten inert gas welding with frequency range of 10-40 kHz on A1050 aluminum alloy. It was also seen that No. of blow holes decreased with decreasing frequency less than 15 kHz. It was

also concluded that sonic wave effect of high frequency caused the decrease in blow holes.

Objective of the present work is to explore weldability on aluminium alloy through TIG welding by varying current, AC frequency and stand-off distance. Effect of these on weld bead geometry is to be found out experimentally.

2.0 EXPERIMENTAL DETAIL

Experiment is performed on Al 1000 series aluminum flat. The TIG welding set up showing the torch with the height adjustment device is shown in Fig. 1. The workpiece dimension is 300 mm x 150 mm x 6 mm. Chemical composition and hardness of the workpiece is given in Table 1.

Table 2 : Specification of Used Weiding Machine

Welding Machine	Master TIG MLS 3003 ACDC
Make	Kemppi Oy, Finland
Rated power at maximum current	9.2 kVA
Current range	3 - 300 A
Wave balance range	0 to -50
Frequency range	50 Hz to 250 Hz

Table 3 : Details of Experimental conditions

Sl.No.	Welding Current		Welding Frequency		Stand-off distance	
	(A)	Coded Value	(Hz)	Coded Value	(mm)	Coded Value
1	120	-	80	-	3	-
2	120	-	80	-	7	+
3	120	-	120	+	7	+
4	120	-	120	+	3	-
5	160	+	80	-	3	-
6	160	+	80	-	7	+
7	160	+	120	+	7	+
8	160	+	120	+	3	-
9	140	0	100	0	5	0
10	140	0	100	0	5	0
11	140	0	100	0	5	0
12	140	0	100	0	5	0
13	140	0	100	0	5	0
14	140	0	100	0	5	0

Detailed specification of the welding machine used is given in **Table 2**. The experimental conditions are given in **Table 3**. Response Surface Methodology (RSM) using Central Composite Design (CCD) is used for selecting the conditions of the experimental runs, or treatments, which facilitate for analyzing the effect of process parameters. The experimental procedure is given below.

Bead-on-plate experiment is performed on Al 1000 series aluminium plates, without filler wire. In this case, depth of penetration and weld bead width are measured. Gas pressure and gas flow rate are set at 15 l/min and 2kg/cm² respectively.

In this experiment, after making 14 bead-on-plate welds on two plates, every weld bead is cut. They are cut in to get 3 pieces each. After that, filing and polishing work by belt grinder/polisher are done. Disc grinder/polisher using different grit sizes of emery papers and then using velvet cloth and alumina paste are employed on the weld cross section of every bead to make it mirror finished. Etching operation is performed on the weld section with the help of 4.5% NaOH (4.5 gm NaOH in 100 ml distilled water) etchant. After etching operation, depth of penetration and bead width are measured by a stereo microscope.

Following constant parameters are set: Gas pressure = 2 kg/cm², Gas flow rate = 15 l/min, Welding speed = 100 mm/min, Electrode diameter = 3 mm, wave balance = -25. No filler is used. Heat input is calculated by the formula:

$$Q = \eta [(60 VI) / (1000 S)] \quad (1)$$

where, Q = heat input (kJ/mm), V = voltage (V), I = current (A), S = welding speed (mm/min) and process efficiency, $\eta = 0.75$.

Etchant is carefully made by mixing 4.5 gm of sodium hydroxide (NaOH) in 100 ml of distilled water. This solution is used after polishing operation, when mirror finish is achieved. In this experiment, the etchant is used for finding out weld bead geometry. The mirror finished sample is immersed within the solution for up to 40 to 50 second. After that bead geometry can be seen.

3.0 RESULTS AND DISCUSSION

Bead-on-plate autogenous welding of Al 1000 series without filler wire is done in these experiments. **Table 3** details the parameters set for this experimental work indicating the coded values for each parameter following CCD type RSM design of experiment. Observations made upon visual test are indicated in **Table 4**. In this experiment, variable AC frequency, AC current, stand-off distance are set at (80 Hz, 100 Hz and 120 Hz), (120 A, 140 A and 160 A) and (3 mm, 5 mm and 7 mm) respectively. Depth of penetration and bead width are measured corresponding to different weld current (I), frequency (f), and stand-off distance (h) at 3 different positions of the work piece and average values are tabulated in **Table 4**. Depth of penetration and bead width are measured at each experimental run using a stereo microscope.

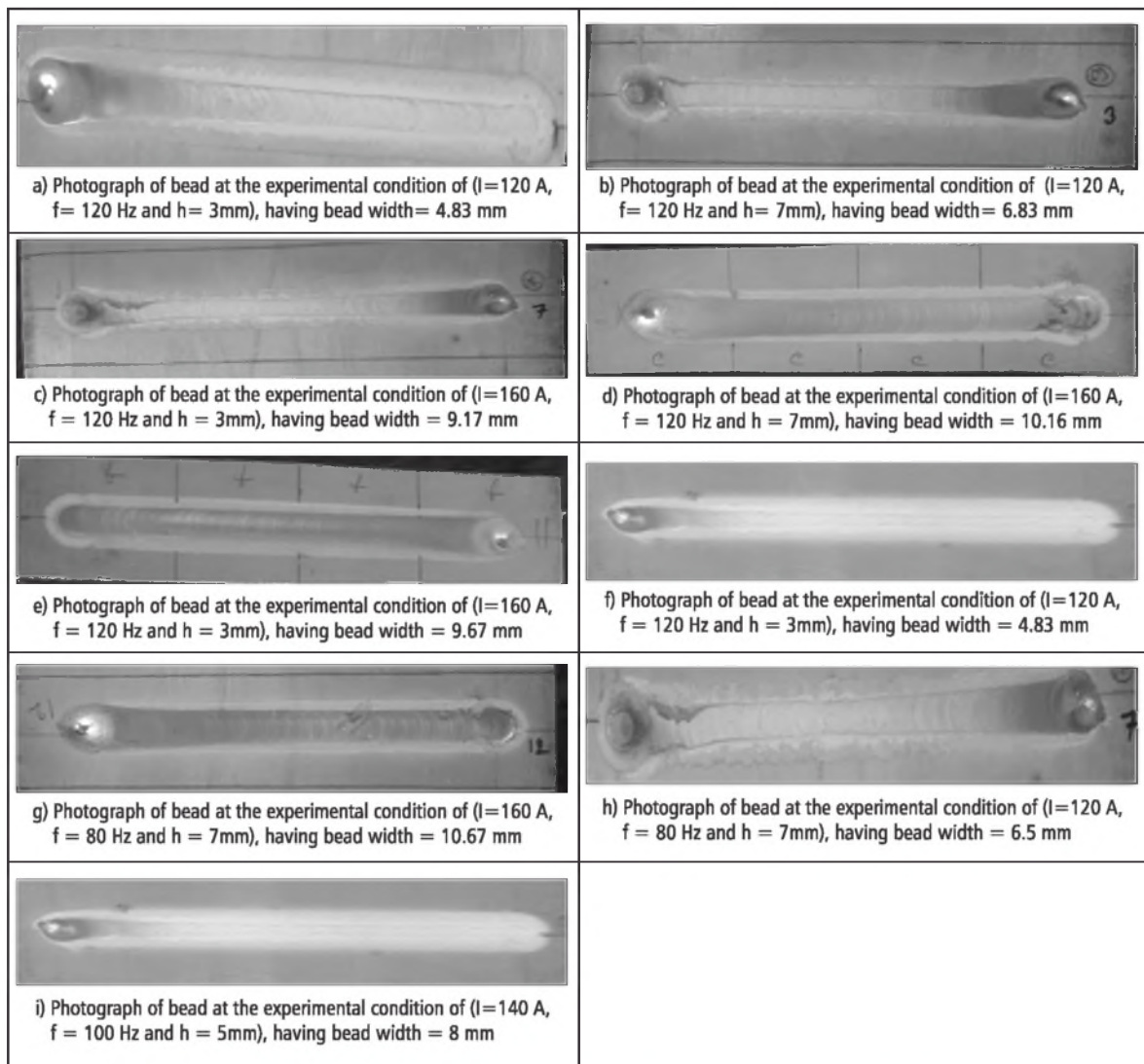


Fig. 2 : Photographs of typical bead-on-plate welded samples

Table 4 : Variation of weld bead width and depth of penetration with different welding current, frequency and stand-off distance

Sl.No.	Run Order	Welding Current (A)	Welding frequency (Hz)	Weld Voltage (V)	Stand-off Distance (mm)	Heat Input (kJ/mm)	Depth of penetration (mm)	Bead width (mm)	Visual Observation of the weld bead
1	2	120	80	16.5	3	0.891	1.791	8	Narrow bead width with porosity
2	3	140	100	16.8	5	1.06	0.86	6.83	Good, uniform welding with few pin holes
3	9	120	120	18.2	7	0.982	2.725	9.17	Narrow bead width with few pin holes
4	13	140	100	16.5	5	1.04	1.06	8	Narrow bead width with some porosity
5	14	120	120	15.5	3	0.837	3.027	10.16	Narrow bead width with porosity
6	1	140	100	17.5	5	1.10	1.598	5.83	Good, uniform bead
7	5	120	80	18	7	0.972	1.15	4.83	Narrow bead width with few pin holes
8	11	140	100	17.5	5	1.10	3.712	9.67	Good, uniform weld
9	4	160	120	16.5	3	1.19	1.747	8	Good, uniform weld
10	7	140	100	17.5	5	1.10	1.483	6.7	Good, uniform weld with few pin holes
11	12	160	80	17.5	3	1.26	3.456	10.67	Good, uniform weld
12	6	160	80	18.8	7	1.35	1.677	8	Good, uniform weld bead
13	8	140	100	17.5	5	1.10	1.747	8	Good, uniform bead with few pin holes
14	10	160	120	18.5	7	1.33	1.556	8	Smooth weld bead

In experimental run Nos. 1-5, 7, 8 and 13, few defects like porosity or pin holes are detected through visual inspection. In other experimental runs, uniform, good weld bead is observed. Overall, quality of welding has been somewhat good with no major welding defect noticed in the test pieces. Fig.2(a-i) represents photographs of typical weld beads formed.

3.1 Variation of Depth of Penetration with the Change in Process Variables

Based on the results obtained, surface and contour plots depicting the variation of depth of penetration with the change

in process variables are made as shown in Fig. 3 through Fig. 8, and analyses are carried out.

Minitab 17 is used for analyzing the data to construct regression model. In this work, influence of the three process variables on depth of penetration is first explored. Equation (2) represents regression Equation for depth of penetration (P) of weld bead.

$$\begin{aligned}
 \text{Penetration, } P = & 28.59 - 0.406 I - 0.339 h - 0.0064 f \\
 & + 0.001638 I^*I + 0.00141 I^*h \\
 & - 0.000108 I^*f + 0.00120 h^*f \quad (2)
 \end{aligned}$$

R² value for this relationship is found out to be 95.72% that is well above 95%, and hence, the regression equation is having a good fit. Therefore, Equation (2) can well be utilized as a predictive model to determine weld penetration at different values of process parameters.

Analysis of variance (ANOVA) is conducted based on the experimental results on depth of penetration and **Table 5** represents the ANOVA table. From this table, it can be clearly seen that p-value for the linear model developed is having 0.000 value indicating the linear model having remarkably significant relationship. Weld current (I) is detected to have p=0.000 value in this equation (2) that means weld current has great influence on penetration. Square of weld current is also seen to be highly significant with a p-value of 0.004. This is expected as high value of current causes high heat input to the

welding process making higher volume of molten weld pool and this often results in deep penetration. Pulse frequency (f) has been found to have significant relation with P as it has a somewhat low p-value of 0.018. However, Negative coefficient of pulse frequency shows decreasing penetration with an increase in pulse frequency. Pulsing also usually causes deep penetration and this observation is also natural. In this case, with an increase in pulse frequency, penetration deteriorates that is also a usual happening in pulsed arc welding process.

However, p-value of stand-off distance (h) and all the 2-way Interaction terms are of more than 50% indicating their insignificant influence on P. On the whole, the regression model developed for penetration has good significance that can also validate the high value of the correlation coefficient, R².

Table 5 : Analysis of variance (ANOVA) table for penetration

Source	DF	Adj SS	Adj MS	F-Value	p-Value
Model	7	9.9807	1.42581	19.17	0.001
Linear	3	8.4509	2.81697	37.88	0.000
Current (I)	1	7.6617	7.66166	103.02	0.000
Stand-off distance (h)	1	0.0161	0.01611	0.22	0.658
Frequency (f)	1	0.7731	0.77315	10.40	0.018
Square	1	1.4711	1.47113	19.78	0.004
I*I	1	1.4711	1.47113	19.78	0.004
2-way Interaction	3	0.0586	0.01955	0.26	0.850
I*h	1	0.0254	0.02543	0.34	0.580
I*f	1	0.0149	0.01488	0.20	0.670
H*f	1	0.0183	0.01834	0.25	0.637
Error	6	0.4462	0.07437		
Lack-of-Fit	1	0.0672	0.06716	0.89	0.390
Pure error	5	0.3791	0.07582		
Total	13	10.4269			

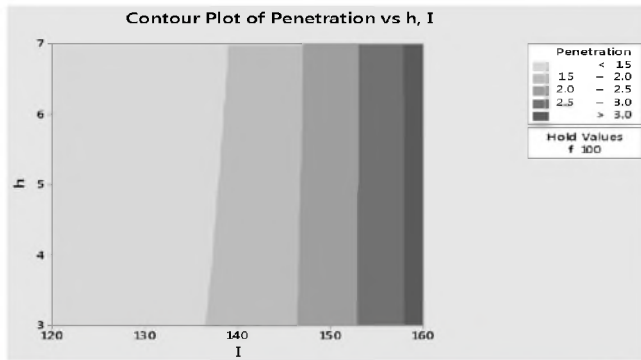


Fig.3 : Contour plot of penetration versus h,i

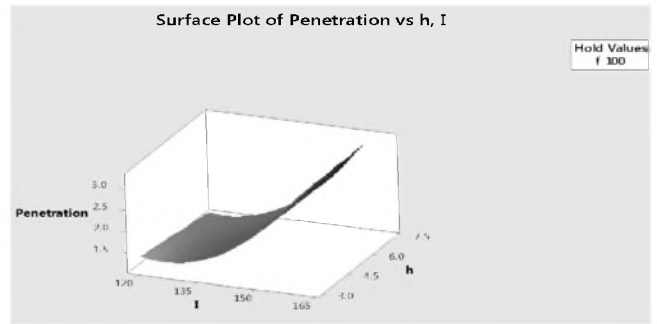


Fig. 4. Surface plot of penetration versus h,i

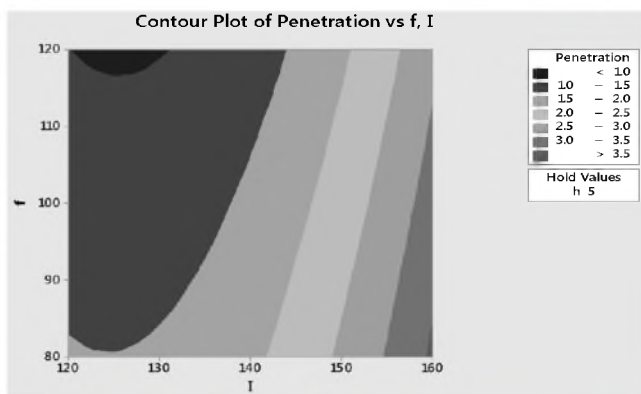


Fig. 5 : Contour plot of penetration versus f, i

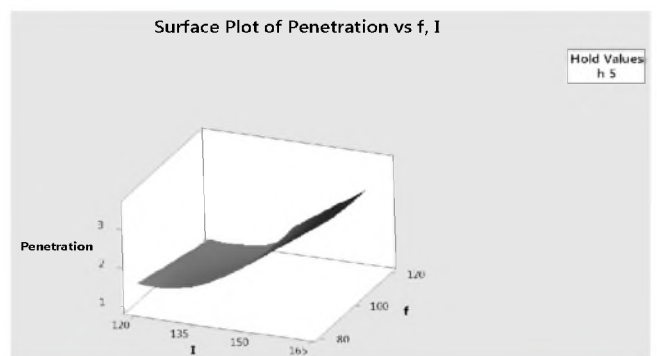


Fig. 6 : Surface plot of penetration versus f, i

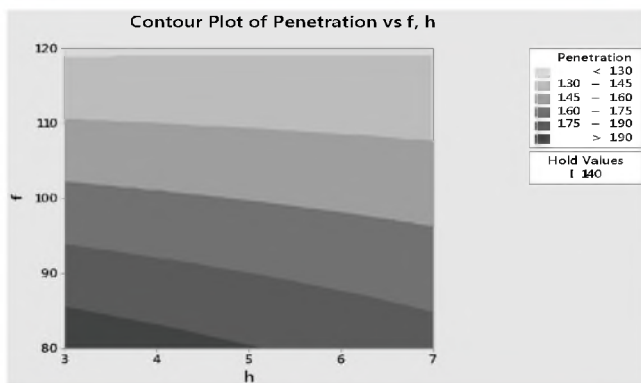


Fig. 7 : Contour plot of penetration versus f, h

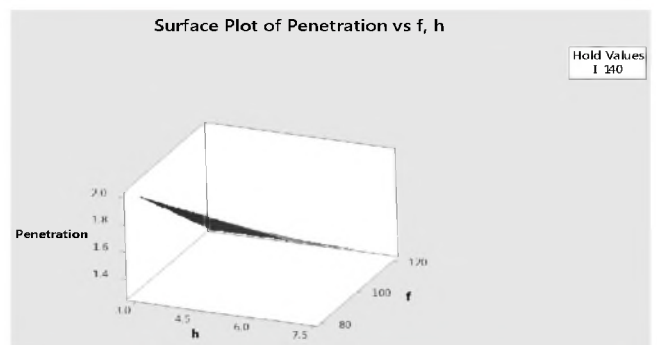


Fig. 8 : Surface plot of penetration versus f, h

Fig. 3 and **Fig. 4** show that depth of penetration increases with the increasing value of current at a hold value of pulse frequency of 100Hz. However, variation of stand-off distance does not affect the penetration. It is also observed from ANOVA **Table 5** that stand-off distance (h) has not been significant for penetration. If stand-off distance increases, higher weld voltage is needed to maintain the arc, and this is likely to cause slight hike in heat input, but the arc may get spread out causing more bead width without penetrating much into the plate to join. From the experimental value, the maximum penetration

depth of 3.712 mm is obtained at a high current of 160 A. This also substantiates the findings that an increase in depth of penetration happens with increasing weld current.

Fig. 5 and **Fig. 6** indicate surface and contour plots of penetration under different current (I) and pulse frequency (f) at a hold value of stand-off distance, h=5 mm. It is also observed here that with the variation of current (I), penetration is increased. If pulse frequency is increased, it decreases penetration, and it is also natural in pulsed arc welding processes.

Contour and surface plots of penetration under different pulse frequency and stand-off distance at a hold current (I) of 140A are shown in Fig. 7 and Fig. 8 respectively. Similar trend in weld bead penetration with pulse frequency and stand-off distance is found as is seen in Fig. 3 through Fig. 6.

3.2 Variation of Bead Width with the Change in Process Variables

Effects of welding current (I), frequency (f) and stand-off distance (h) on bead width (W) are also explored in the present bead-on-plate autogenous welding. Regression analysis is done using Minitab 17 software and a relationship is developed as shown in equation (3). Equation (3) can be utilized as a predictive model to determine the value of bead width at different values of process parameters.

$$\begin{aligned} \text{Bead Width, } W = & -7.53 + 0.1271 I - 0.0231 f + 0.339 h \\ & - 0.000044 I^*I - 0.000044 I^*f \\ & - 0.00275 I^*h + 0.00350 f^*h \end{aligned} \quad (3)$$

R² value of 99.52% is observed in this case. So, the regression

equation evaluated is having quite good fit, and this equation may well be used for estimating bead width effectively.

Effect of parameters on bead width is observed from ANOVA Table 6. ANOVA table shows p-value of 0.000 for the model developed and also for the linear model indicating strong relationship existing in this model within bead width and the process variables. Negative coefficient of pulse frequency shows a decreasing bead width with an increase in pulse frequency. Bead width is found to be strongly influenced by weld current (I) as well as pulse frequency (f) as their p-values are also 0.000. This means high current and low pulse frequency are likely to result in high volume of molten weld pool causing not only increase in penetration, but also hikes bead width. In this case, stand-off distance (h) is also detected to be having much influence on bead width. As the stand-off distance (h) increases, concentrated arc is difficult to get and the arc gets spread out resulting in more bead width as a usual fact. Few interaction or square terms have more than p-value of 0.50 indicating insignificant relationship; however, some other terms have significance to some extent.

Table 6 : Analysis of variance (ANOVA) table for bead width

Source	DF	Adj SS	Adj MS	F-Value	p-Value
Model	7	33.6051	4.8007	177.31	0.000
Linear	3	33.3481	11.1160	410.56	0.000
Current (I)	1	29.9538	29.9538	1106.33	0.000
Stand-off distance (h)	1	0.4418	0.4418	16.32	0.007
Frequency (f)	1	2.9525	2.9525	109.05	0.000
Square	1	0.0010	0.0010	0.04	0.850
I*I	1	0.0010	0.0010	0.04	0.850
2-way Interaction	3	0.2561	0.0854	3.15	0.108
I*h	1	0.0025	0.0025	0.09	0.774
I*f	1	0.0968	0.0968	3.58	0.108
H*f	1	0.1568	0.1568	5.79	0.053
Error	6	0.1624	0.0271		
Lack-of-Fit	1	0.1624	0.1624		
Pure error	5	0.0000	0.0000		
Total	13	33.7676			

Variation of bead width with different levels of process variables can be observed from Fig. 9 through Fig. 14. The nature of contour plot and surface plot can be followed as shown in Fig. 9 through Fig. 14. Fig. 9 and Fig. 10 are the contour plot and surface plot of bead width with the variation of

pulse frequency (f) and weld current (I) at a hold value of stand-off distance of 5mm. As indicated by the ANOVA table, these plots also show clear effect of current on bead width. Frequency on the other hand, has small influence on bead width compared to that of current.

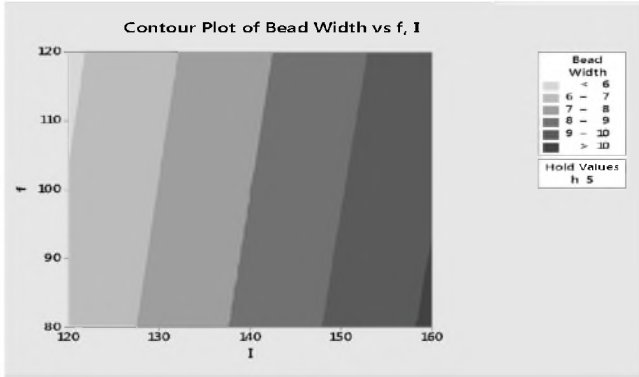


Fig. 9 : Contour plot of bead width versus f, I

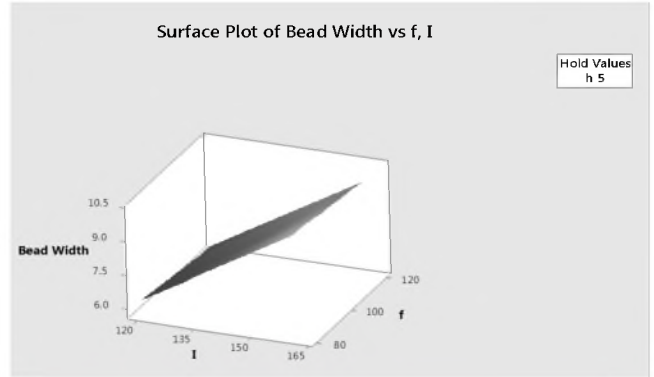


Fig.10 : Surface plot of bead width versus f, I

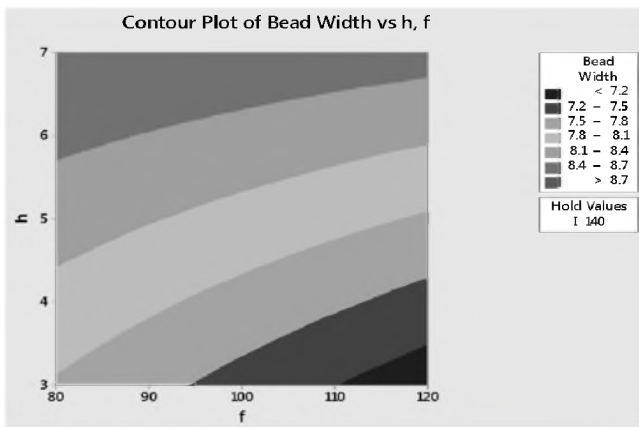


Fig. 11 : Contour plot of bead width versus h, f

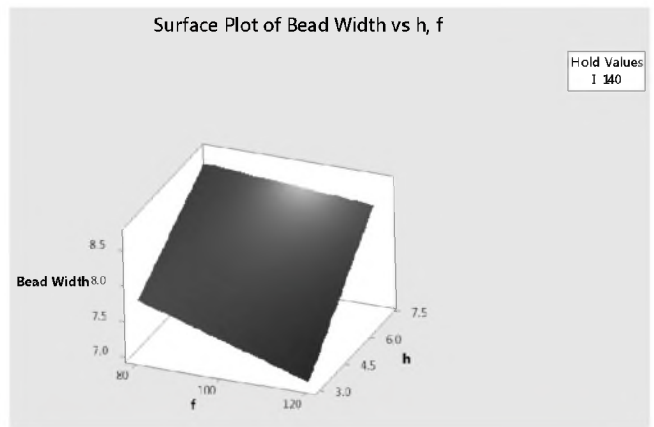


Fig. 12 : Surface plot of bead width versus h, f

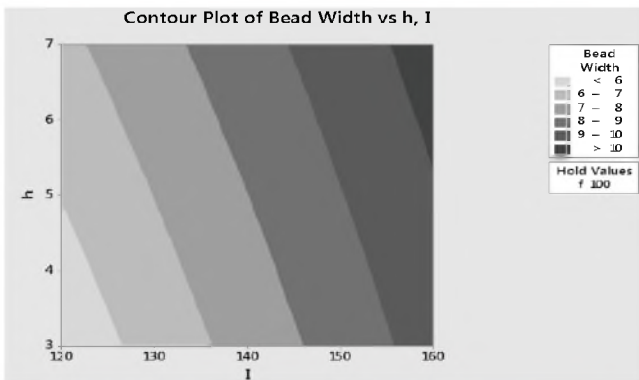


Fig. 13 : Contour plot of bead width versus h, I

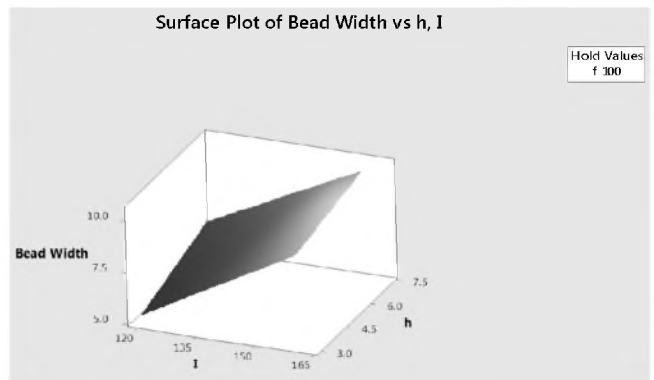


Fig. 14 : Contour plot of bead width versus h, I

In the contour plot, **Fig. 11** and surface plot, **Fig. 12**, variation of weld bead width under different frequency (f) and stand-off distance (h) at a constant current (I) at a hold value of 140 A is represented. Both the figures show the variation of bead width with respect to stand-off distance and frequency. It can be seen that weld bead width is increased with increase in stand-off distance, whereas, if there is an increase in frequency, weld bead width is showing a decreasing tendency.

Fig. 13 and **Fig. 14** depict surface plot and contour plot of bead width with the variation of stand-off distance (h) and current (I) at a hold value of frequency (f) of 100 Hz. As expected, increase in current increases bead width at a higher rate, and increase in stand-off distance also causes a hike in bead width, but with a lower magnitude than that of current.

Finally it can be stated that weld current influences the most bead penetration as well as bead width; stand-off distance has an effect on increasing bead width. Pulsing frequency at a low level tends to increase penetration as well as width of weld bead albeit at a low extent.

4.0 CONCLUSIONS

From the above observations on experimental results, following conclusions can be drawn:

1. Increase in welding current increases weld penetration significantly. It also increases bead width to some extent. It is expected as hike in weld current results in increase in heat input and hence, the volume of molten weld pool.
2. More the stand-off distance, higher is the weld bead width. This is natural as increased stand-off distance causes more spreading of the arc thereby increasing width of weld bead.
3. Pulse frequency, if increased, causes a decrease in weld penetration as well as weld bead width.
4. Finally, high weld current, low pulse frequency and low stand-off distance can be recommended for having deep penetration of the weld bead.

REFERENCES

1. Kinsey, B. and Viswanathan, V. and Cao, J. (2001); Forming of aluminum tailor welded blanks, SAE Technical Paper
2. Tusek J., Kampus Z. and Suban M. (2001); Welding of tailored blanks of different materials, Journal of Materials Processing Technology, 119, pp.180-184.
3. Arunkumar D. and Subbaiah K. (2019); Effect of Continuous and Pulsed Current Tungsten Inert Gas Welding of Cast Al–Mg–Sc Alloy, Springer Nature Singapore Pte Ltd, pp. 653-662.
4. Ding D. and Wang Y. W. (2013); Effects of post weld heat treatment on properties of variable polarity TIG welded AA2219 aluminium alloy joints, Transactions of Nonferrous Metals society China, 24, pp. 1307-1316.
5. Kumar T. S., Balasubramanian V. and Sanavullah M. Y. (2006); Influences of pulsed current tungsten inert gas welding parameters on the tensile properties of AA 6061 aluminium alloy, Materials and Design, 28, pp. 2080-2092.
6. Reddy G. M., Gokhale A. A. and Prasad Rao K. (1997); Optimisation of pulse frequency in pulsed current gas tungsten arc welding of aluminum-lithium alloy sheets, Materials Science and Technology, 14, pp. 61-66.
7. Lothongkum G., Chaumbai P. and Bhandhubanyong P. (1999); TIG pulse welding of 304L austenitic stainless steel in flat, vertical and overhead positions, Journal of Materials Processing Technology, 89-90, pp. 410-414.
8. Guang-jun Z., Zhi-hong Y. and Lin W. (2006); Visual sensing of weld pool in variable polarity TIG welding of aluminum alloy, Transaction Nonferrous Metals Society China, 16, pp. 522- 526.
9. Mohan P. (2014); Study the effects of welding parameters on TIG welding of aluminum plates, A thesis submitted to Department of Mechanical Engineering National Institute of Technology Rourkela
10. Potluri N.B., Ghosh P.K. and Gupta P.C. (1996); Studies on weld metal characteristics and their influence on tensile and fatigue properties of pulsed – current GMA welded Al-Zn-Mg alloy, Welding Journal, 75, pp. 62-70.
11. Ghosh, N. and Das, S. (2019); Study on effect of welding parameters on weld bead geometry of AC TIG welding in aluminium, Manufacturing Technology Today, Vol.18, No.9, pp.30-38.
12. Ming, L. Q., Xin-hong, W., da, Z. Z. and Jun, W. (2007); Effect of activating flux on arc shape and arc voltage in tungsten inert gas welding, Transaction Nonferrous Metals Society China, 17, pp. 486 – 490.
13. Morisada Y., Fujii H., Inagaki F. and Kamai M. (2013); Development of high frequency tungsten inert gas welding method, Materials and Design, 44, pp. 12-16.